Hindawi
Journal of Chemistry
Volume 2020, Article ID 6181356, 8 pages
https://doi.org/10.1155/2020/6181356

Research Article

Heat Capacities and Thermodynamic Properties of Pinnoite and Inderite

Hanyu Zheng, Kangrui Sun, Long Li, Yafei Guo, and Tianlong Deng

Tianjin Key Laboratory of Marine Resources and Chemistry, College of Chemical Engineering and Materials Science, Tianjin University of Science and Technology, Tianjin 300457, China

Correspondence should be addressed to Yafei Guo; guoyafei@tust.edu.cn and Tianlong Deng; tldeng@tust.edu.cn

Received 13 November 2019; Accepted 25 January 2020; Published 10 March 2020

Academic Editor: Saima Q. Memon

Copyright © 2020 Hanyu Zheng et al. This is an open access article distributed under the Creative Commons Attribution License, which permits unrestricted use, distribution, and reproduction in any medium, provided the original work is properly cited.

In this paper, in order to understand the thermodynamic properties of natural minerals of pinnoite ($MgB_2O_4{\cdot}3H_2O$, Pin) and inderite ($Mg_2B_6O_{11}{\cdot}15H_2O$, Ind) deposited in salt lakes, heat capacities of two minerals were measured using a precision calorimeter at temperatures from 306.15 to 355.15 K after the high purity was synthesized. It was found that there are no phase transitions and thermal anomalies for the two minerals, and the molar heat capacities against temperature for Pin and Ind were fitted as $C_{p,m,pin} = -2029.47058 + 16.94666T - 0.04396T^2 + 3.89409\times10^{-5}T^3$ and $C_{p,m,Ind} = -30814.43795 + 282.68108T - 0.85605T^2 + 8.70708\times10^{-4}T^3$, respectively. On the basis of molar heat capacities ($C_{p,m}$) of Pin and Ind, the thermodynamic functions of entropy, enthalpy, and Gibbs free energy at the temperature of 1 K interval for the two minerals were obtained for the first time.

1. Introduction

Magnesium borates are widely used in many fields such as chemical industry, glass and ceramics industries, and superconducting materials because of the excellent performance [1–4], and the extensive application of magnesium borate also makes it a great resource to be developed and utilized in the world today. Fortunately, six natural hydrated magnesium borate minerals $2MgO{\cdot}3B_2O_3{\cdot}15H_2O$ (inderite), $2MgO{\cdot}3B_2O_3{\cdot}15H_2O$ (kurnakovite), $2MgO{\cdot}2B_2O_3{\cdot}MgCl_2{\cdot}14H_2O$ (chloropinnoite), $MgO{\cdot}B_2O_3{\cdot}3H_2O$ (pinnoite), $MgO{\cdot}2B_2O_3{\cdot}9H_2O$ (hungchaoite), and $MgO{\cdot}3B_2O_3{\cdot}7.5H_2O$ (mcallisterite) have been found in the Qaidam Basin, China [5, 6]. It is well known that thermodynamic properties are the theoretical foundation for the exploitation of brine resources; hence, in order to provide useful information for synthesizing materials and extracting magnesium borates in salt lake brines, the study of thermodynamic properties for magnesium borates is necessary.

Heat capacity which refers to the energy absorbed or released when the unit mass changes per unit temperature [7] is one of the important thermodynamic properties for optimizing the production process, and it can be used for reliable calculation of enthalpy, entropy, and Gibbs free energy [8, 9]. In addition, heat capacity is the inherent characteristic of crystals, which is closely related to its unique composition and crystal structure. In order to understand the thermodynamic properties of natural minerals of pinnoite ($MgB_2O_4{\cdot}3H_2O$, Pin) and inderite ($Mg_2B_6O_{11}{\cdot}15H_2O$, Ind) deposited in salt lakes, the heat capacities of minerals pinnoite and inderite were measured using the calorimeter at temperatures from 306.15 to 355.15 K after the high purity was synthesized [10], and the relative thermodynamic functions of entropy, enthalpy, and Gibbs free energy were also carried out according to the thermodynamic equations for the first time.

2. Experimental

2.1. Recrystallizations or Synthesizations and Characterizations for Pinnoite and Inderite. For pinnoite purification, 30.00 g of the $MgB_2O_4{\cdot}H_2O$ purchased products was taken and dissolved in 100.00 g of fresh CO_2-free deionized distilled water (DDW), and the pH was adjusted to 8 with 50% (v/v) hydrochloric acid, and then, the solution was stirred at 200 rpm for about one week at room temperature until the solution reaches equilibrium. Next, the precipitates were filtered and washed with DDW three times as well as once with anhydrous

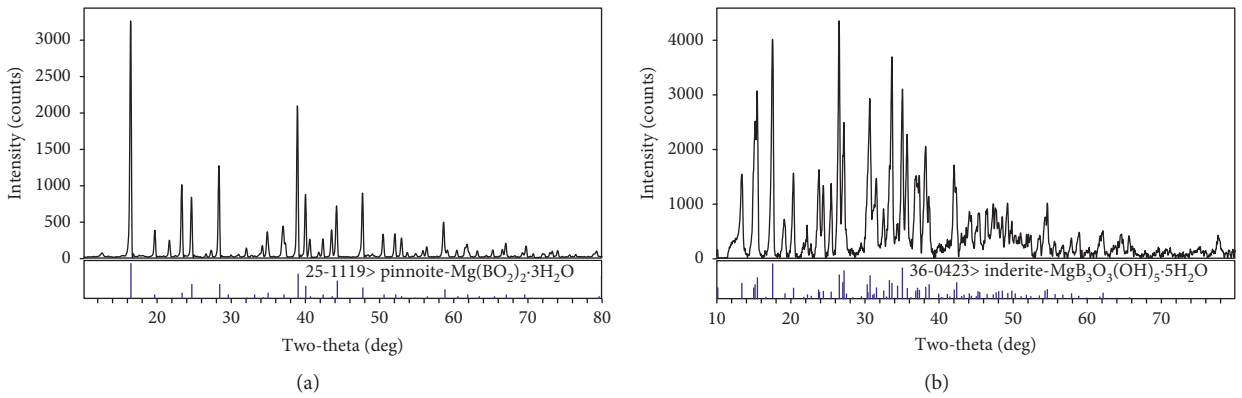

Figure 1: The X-ray diffraction patterns of pinnoite (a) and inderite (b).

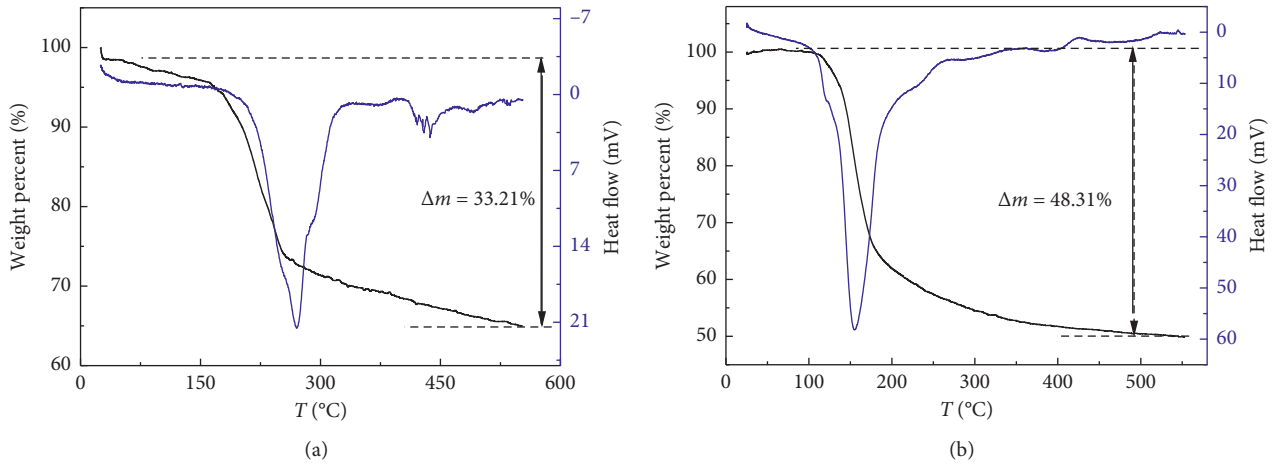

Figure 2: The TG-DSC curves of pinnoite (a) and inderite (b).

ethanol and then dried at 25°C in a vacuum drying box and characterized before use. The synthesis of inderite was done as described previously [11, 12]. Briefly, 40.00 g borax was dissolved in 400.00 g of fresh CO_2-free deionized distilled water (DDW) under the condition of stirring at 343.15 K. After the borax dissolved completely, the temperature was decreased to 323.15 K to add 40.00 g of $MgSO_4{\cdot}7H_2O$, and then the solution was stirred at 200 rpm for 12 hours. The precipitate was filtered in attemperator and then recrystallized in a thermostat water bath at 303 K. Similarly, it was filtered in an attemperator and washed three times with DDW and once with anhydrous ethanol and then dried in a desiccator before use.

The pinnoite and inderite were identified by X-ray diffraction analysis (MSAL XD-3, Beijing Purkinje General Instrument Co. Ltd., China), and the results are shown in Figure 1, and it showed that the diffraction peaks on patterns correspond well with the standard Atlas database. Figure 2 shows the method for the identification of pinnoite and inderite by TG-DSC (Labsys, Setaram, France), respectively. The thermal analysis curve results of pinnoite showed that the total weight loss rate of the sample is 33.21% between 378.15 K and 813.15 K, which is basically consistent with the theoretical loss of water from $MgB_2O_4{\cdot}3H_2O$ to MgB_2O_4 (32.96%) [13], and the deviation is within 0.05%. From the thermal analysis curve of inderite, it was found that the sample had a continuous weightlessness section between 373.15 K and 673.15 K, and the total weight loss rate was 48.31%, which was basically consistent with the theoretical water loss rate of 48.29% of $Mg_2B_6O_{11}{\cdot}15H_2O$ from hot loss of crystalline water to $Mg_2B_6O_{11}$. The concentration of borate expressed as B_2O_3 was analyzed by the gravimetric methods of mannitol with an uncertainty of ±0.0005 in mass fraction [14]. The content of magnesium expressed as MgO in the sample was determined by EDTA complexometry with an uncertainty of ±0.0051 in mass fraction, and the content of H_2O can be calculated by subtraction. The analytical results of $MgB_2O_4{\cdot}3H_2O$ and $Mg_2B_6O_{11}{\cdot}15H_2O$ were compared with the theoretical values and are shown in Table 1, and it was shown that the purities of the synthesized pinnoite and inderite were higher than 99.9%.

2.2. Experimental Method. The high-precision calorimeter (Labsys, Setaram, France) was used for heat capacity experiment, which requires three groups of minerals, namely, blank, reference, and sample experiments, and alumina as a reference experiment. To verify the performance, the heat capacity of KCl was measured, and the average experimental value for five times of 0.6860 $J{\cdot}g^{-1}{\cdot}K^{-1}$ is in accordance with 0.6879 $J{\cdot}g^{-1}{\cdot}K^{-1}$ reported in the literature [15], and the deviation is 0.0028. The

Table 1: Chemical analytical results of pinnoite ($MgB_2O_4{\cdot}3H_2O$) and inderite ($Mg_2B_6O_{11}{\cdot}15H_2O$)[a].

Component content	Purity	w (MgO)	w (B_2O_3)	w (H_2O)	n (MgO: B_2O_3: H_2O)
Pinnoite ($MgB_2O_4{\cdot}3H_2O$)					
Theoretical	1.0000	0.2459	0.4247	0.3274	1.00: 1.00: 3.00
Experimental	0.9920	0.2447	0.4243	0.3300	1.00: 1.00: 3.01
Inderite ($Mg_2B_6O_{11}{\cdot}15H_2O$)					
Theoretical	1.0000	0.1440	0.3732	0.4828	2.00:3.00:15.00
Experimental	0.9990	0.1439	0.3734	0.4827	2.00:3.00:15.02

[a]Standard uncertainties u are u(MgO) = 0.0051, u(B_2O_3) = 0.0005, and u(H_2O) = 0.0079 in mass fraction.

Table 2: The molar heat capacities of pinnoite and inderite at 306.15~355.15 K[a].

T (K)	$C_{p,m}$ ($J{\cdot}mol^{-1}{\cdot}K^{-1}$)	T (K)	$C_{p,m}$ ($J{\cdot}mol^{-1}\,K^{-1}$)	T (K)	$C_{p,m}$ ($J{\cdot}mol^{-1}\,K^{-1}$)
Pinnoite, $MgB_2\,O_4\cdot3H_2\,O$					
306.15	154.85	323.15	169.84	340.15	181.16
307.15	155.94	324.15	170.55	341.15	181.66
308.15	157.45	325.15	171.22	342.15	182.19
309.15	158.71	326.15	171.93	343.15	182.68
310.15	159.85	327.15	172.60	344.15	183.16
311.15	160.76	328.15	173.30	345.15	183.63
312.15	161.68	329.15	173.96	346.15	184.09
313.15	162.60	330.15	174.65	347.15	184.53
314.15	163.39	331.15	175.37	348.15	184.96
315.15	164.14	332.15	176.07	349.15	185.40
316.15	164.88	333.15	176.80	350.15	185.86
317.15	165.52	334.15	177.57	351.15	186.34
318.15	166.17	335.15	178.27	352.15	186.86
319.15	166.84	336.15	178.91	353.15	187.43
320.15	167.57	337.15	179.53	354.15	188.04
321.15	168.32	338.15	180.09	355.15	188.70
322.15	169.07	339.15	180.63		
Inderite, $Mg_2B_6O_{11}{\cdot}15H_2O$					
306.15	474.94	323.15	521.82	340.15	560.43
307.15	479.69	324.15	524.12	341.15	562.89
308.15	484.73	325.15	526.36	342.15	565.29
309.15	488.20	326.15	528.59	343.15	567.98
310.15	490.94	327.15	530.77	344.15	570.78
311.15	493.51	328.15	533.01	345.15	573.30
312.15	495.98	329.15	535.19	346.15	576.09
313.15	498.44	330.15	537.38	347.15	578.95
314.15	500.45	331.15	539.50	348.15	581.91
315.15	502.52	332.15	541.57	349.15	584.65
316.15	504.70	333.15	543.75	350.15	587.56
317.15	506.89	334.15	545.82	351.15	590.97
318.15	509.24	335.15	548.06	352.15	595.06
319.15	511.70	336.15	550.52	353.15	600.09
320.15	514.21	337.15	552.93	354.15	605.63
321.15	516.73	338.15	555.50	355.15	611.12
322.15	519.25	339.15	557.97		

[a]The sample weights for pinnoite and inderite were 15.92 and 15.27 mg, respectively. The temperature heating rate was 2 $K{\cdot}min^{-1}$. The standard uncertainty u is u ($C_{p,m}$) = 0.05 $J{\cdot}mol^{-1}{\cdot}K^{-1}$.

heat capacities of the samples were carried out in the range of 306.15 K to 355.15 K with a heating rate of 2 K/min, putting about 15 mg of samples in the crucible weighted with an accuracy of 0.00001 g, and the flow rate of N_2 is 20 mL/min.

3. Results and Discussion

3.1. Measurement of the Heat Capacity. The values for the molar heat capacities of pinnoite and inderite were measured by the calorimeter at temperature from 306.15 to 355.15 K with the standard uncertainty of 0.05 $J{\cdot}mol^{-1}{\cdot}K^{-1}$ are listed in Table 2 and plotted in Figure 3 [16]. As shown in Figure 3, the heat capacities of pinnoite and inderite are all increased with the rise of temperature from 306.15 to 355.15 K, which shows that the structures of pinnoite and inderite are stable in these temperature regions, that is, neither phase transition nor other thermal anomalies take place within the temperature range of the experiment.

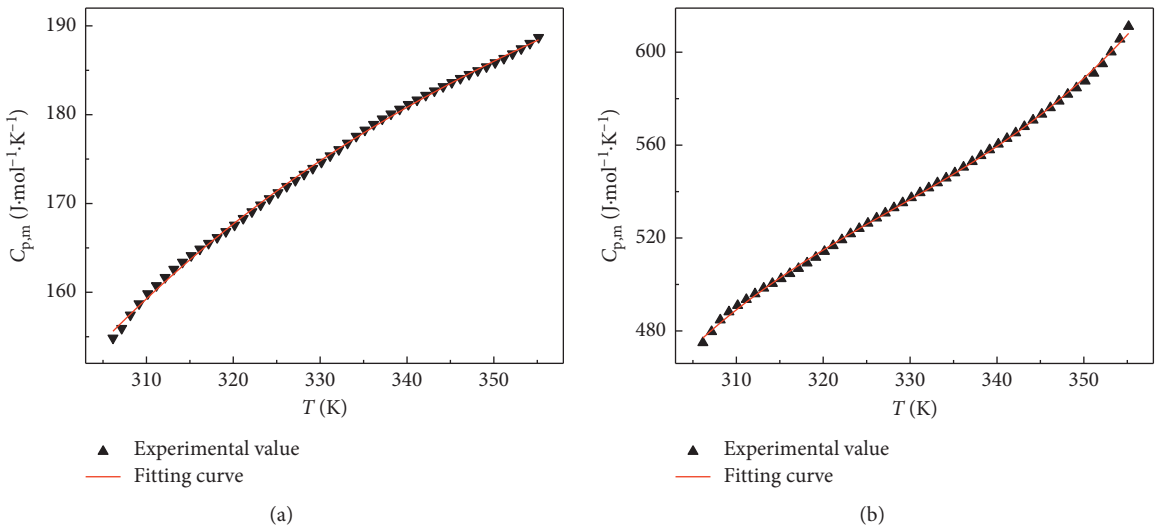

Figure 3: Molar heat capacities versus temperature in the range of 306.15 K to 355.15 K for pinnoite (a) and inderite (b).

Table 3: Polynomial coefficients of equation (1) for minerals of pinnoite and inderite at 306.15~355.15 K.

Minerals	Polynomial coefficient				r
	A_0	A_1	A_2	A_3	
$MgB_2O_4{\cdot}3H_2O$	−2029.47058	16.94666	−0.04396	3.89409×10^{-5}	0.99905
$Mg_2B_6O_{11}{\cdot}15H_2O$	−30814.43795	282.68108	−0.85605	8.70708×10^{-4}	0.99924

Table 4: Molar heat capacities and thermodynamic functions $(H_T - H_{298.15})$, $(S_T - S_{298.15})$, and $(G_T - G_{298.15})$ of pinnoite and inderite.

T (K)	$C^a_{p,m}$ (J·mol^{-1}·K^{-1})	$H_T - H^a_{298.15}$ (kJ·mol^{-1})	$S_T - S^a_{298.15}$ (J·mol^{-}·K^{-1})	$G_T - G^a_{298.15}$ (kJ·mol^{-1})
Pinnoite, $MgB_2O_4{\cdot}3H_2O$				
298.15	147.49	0.0000	0.0000	0.0000
306.15	154.85	1.2142	4.0183	−0.0160
307.15	155.94	1.3706	4.5282	−0.0203
308.15	157.45	1.5279	5.0396	−0.0251
309.15	158.71	1.6862	5.5524	−0.0303
310.15	159.85	1.8454	6.0665	−0.0362
311.15	160.76	2.0055	6.5820	−0.0425
312.15	161.68	2.1665	7.0986	−0.0493
313.15	162.60	2.3284	7.6165	−0.0567
314.15	163.39	2.4912	8.1355	−0.0646
315.15	164.14	2.6548	8.6555	−0.0730
316.15	164.88	2.8193	9.1766	−0.0819
317.15	165.52	2.9846	9.6986	−0.0913
318.15	166.17	3.1507	10.2215	−0.1013
319.15	166.84	3.3176	10.7453	−0.1117
320.15	167.57	3.4853	11.2700	−0.1228
321.15	168.32	3.6538	11.7954	−0.1343
322.15	169.07	3.8230	12.3215	−0.1463
323.15	169.84	3.9930	12.8483	−0.1589
324.15	170.55	4.1637	13.3758	−0.1720
325.15	171.22	4.3352	13.9039	−0.1857
326.15	171.93	4.5073	14.4325	−0.1999
327.15	172.60	4.6802	14.9616	−0.2145
328.15	173.30	4.8537	15.4913	−0.2298
329.15	173.96	5.0279	16.0213	−0.2455
330.15	174.65	5.2028	16.5518	−0.2618
331.15	175.37	5.3783	17.0827	−0.2786
332.15	176.07	5.5545	17.6139	−0.2960
333.15	176.80	5.7313	18.1453	−0.3139

Table 4: Continued.

T (K)	$C^{a}_{p,m}$ (J·mol^{-1}·K^{-1})	$H_T - H^{a}_{298.15}$ (kJ·mol^{-1})	$S_T - S^{a}_{298.15}$ (J·mol^{-}·K^{-1})	$G_T - G^{a}_{298.15}$ (kJ·mol^{-1})
334.15	177.57	5.9087	18.6771	−0.3323
335.15	178.27	6.0867	19.2091	−0.3512
336.15	178.91	6.2654	19.7413	−0.3707
337.15	179.53	6.4446	20.2737	−0.3907
338.15	180.09	6.6244	20.8063	−0.4112
339.15	180.63	6.8048	21.3389	−0.4323
340.15	181.16	6.9857	21.8717	−0.4539
341.15	181.66	7.1673	22.4045	−0.4761
342.15	182.19	7.3493	22.9374	−0.4987
343.15	182.68	7.5319	23.4703	−0.5219
344.15	183.16	7.7151	24.0033	−0.5457
345.15	183.63	7.8987	24.5361	−0.5699
346.15	184.09	8.0829	25.0690	−0.5947
347.15	184.53	8.2676	25.6018	−0.6201
348.15	184.96	8.4528	26.1345	−0.6459
349.15	185.40	8.6385	26.6671	−0.6723
350.15	185.86	8.8246	27.1995	−0.6993
351.15	186.34	9.0113	27.7319	−0.7267
352.15	186.86	9.1985	28.2641	−0.7547
353.15	187.43	9.3861	28.7961	−0.7833
354.15	188.04	9.5742	29.3279	−0.8123
355.15	188.70	9.7627	29.8596	−0.8419
Inderite, $Mg_2B_6O_{11}{\cdot}15H_2O$				
298.15	446.59	0.0000	0.0000	0.0000
306.15	474.94	3.7018	12.2505	−0.0487
307.15	479.69	4.1809	13.8128	−0.0617
308.15	484.73	4.6632	15.3806	−0.0763
309.15	488.20	5.1487	16.9535	−0.0925
310.15	490.94	5.6372	18.5311	−0.1102
311.15	493.51	6.1287	20.1131	−0.1295
312.15	495.98	6.6230	21.6992	−0.1504
313.15	498.44	7.1201	23.2891	−0.1729
314.15	500.45	7.6198	24.8825	−0.1970
315.15	502.52	8.1222	26.4791	−0.2227
316.15	504.70	8.6271	28.0788	−0.2500
317.15	506.89	9.1345	29.6812	−0.2789
318.15	509.24	9.6444	31.2862	−0.3093
319.15	511.70	10.1566	32.8937	−0.3414
320.15	514.21	10.6711	34.5034	−0.3751
321.15	516.73	11.1880	36.1152	−0.4104
322.15	519.25	11.7070	37.7290	−0.4474
323.15	521.82	12.2283	39.3446	−0.4859
324.15	524.12	12.7518	40.9621	−0.5260
325.15	526.36	13.2775	42.5812	−0.5678
326.15	528.59	13.8053	44.2019	−0.6112
327.15	530.77	14.3352	45.8243	−0.6562
328.15	533.01	14.8673	47.4482	−0.7029
329.15	535.19	15.4015	49.0737	−0.7511
330.15	537.38	15.9378	50.7008	−0.8010
331.15	539.50	16.4764	52.3294	−0.8525
332.15	541.57	17.0170	53.9596	−0.9057
333.15	543.75	17.5599	55.5916	−0.9604
334.15	545.82	18.1050	57.2252	−1.0169
335.15	548.06	18.6523	58.8607	−1.0749
336.15	550.52	19.2019	60.4981	−1.1346
337.15	552.93	19.7538	62.1375	−1.1959
338.15	555.50	20.3081	63.7791	−1.2588
339.15	557.97	20.8648	65.4230	−1.3235
340.15	560.43	21.4239	67.0693	−1.3897
341.15	562.89	21.9857	68.7183	−1.4576

Table 4: Continued.

T (K)	$C^{a}_{p,m}$ (J·mol^{-1}·K^{-1})	$H_T - H^{a}_{298.15}$ (kJ·mol^{-1})	$S_T - S^{a}_{298.15}$ (J·mol^{-}·K^{-1})	$G_T - G^{a}_{298.15}$ (kJ·mol^{-1})
342.15	565.29	22.5500	70.3701	−1.5271
343.15	567.98	23.1170	72.0248	−1.5983
344.15	570.78	23.6867	73.6828	−1.6712
345.15	573.30	24.2593	75.3442	−1.7457
346.15	576.09	24.8349	77.0092	−1.8219
347.15	578.95	25.4134	78.6782	−1.8997
348.15	581.91	25.9951	80.3514	−1.9792
349.15	584.65	26.5800	82.0290	−2.0604
350.15	587.56	27.1682	83.7113	−2.1433
351.15	590.97	27.7599	85.3987	−2.2278
352.15	595.06	28.3552	87.0914	−2.3141
353.15	600.09	28.9541	88.7898	−2.4020
354.15	605.63	29.5569	90.4942	−2.4917
355.15	611.12	30.1636	92.2050	−2.5830

[a]The standard uncertainties u are $u\,(C_{p,m}) = 0.05$ J·mol^{-1}·K^{-1}, $u(H_T - H_{298.15}) = 0.0056$, $u(S_T - S_{298.15}) = 0.0080$, and $u(G_T - G_{298.15}) = 0.0010$.

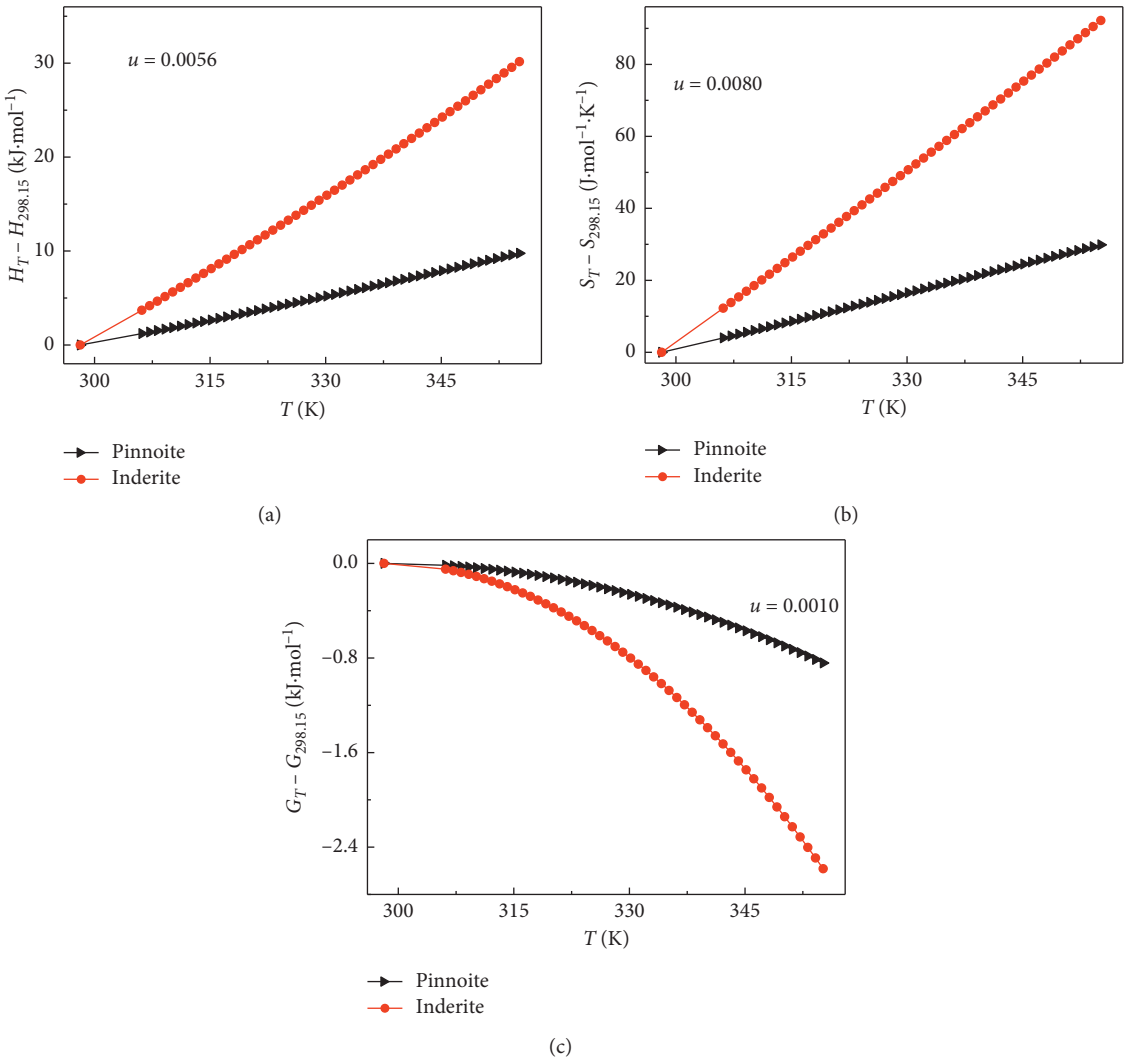

Figure 4: Variations of (a) $(H_T - H_{298.15})$, (b) $(S_T - S_{298.15})$, and (c) $(G_T - G_{298.15})$ with T for pinnoite and inderite.

In order to obtain the heat capacity quickly at a certain temperature, the molar heat capacities of pinnoite and inderite determined in this work have been fitted as equation (1) by means of a least-squares method with the correlation coefficients $r = 0.99905$ for pinnoite and 0.99924 for inderite listed in Table 3. On the basis of polynomial equations, the

molar heat capacities of pinnoite and inderite at 298.15 K can be calculated as 147.49 and 446.59 $J \cdot mol^{-1} \cdot K^{-1}$, and the standard deviations between experimental values $C_{p,exp}$ and fitted values $C_{p,fit}$ through the polynomial equation are within 0.02:

$$C_{p,m}\left(J \cdot mol^{-1} \cdot K^{-1}\right) = A_0 + A_1 T + A_2 T^2 + A_3 T^3. \quad (1)$$

3.2. Enthalpy, Entropy, and Gibbs Free Energy. The thermodynamic functions of the relative standard states of pinnoite and inderite at 298.15 K can be derived from the following thermodynamic equations:

$$H_T - H_{298.15} = \int_{298.15}^{T} C_{p,m} dT,$$

$$S_T - S_{298.15} = \int_{298.15}^{T} \left[\frac{C_{p,m}}{T}\right] dT, \quad (2)$$

$$G_T - G_{298.15} = \int_{298.15}^{T} C_{p,m} dT - T \int_{298.15}^{T} \left[\frac{C_{p,m}}{T}\right] dT.$$

Using the formula above, the thermodynamic functions $(H_T - H_{298.15})$, $(S_T - S_{298.15})$, and $(G_T - G_{298.15})$ of pinnoite and inderite are calculated on the basis of the obtained heat capacity values and are listed in Table 4 with a temperature of 1 K interval.

From the thermodynamic function data listed in Table 4, it is shown that with the increase of temperature from 298.15 K to 355.15 K, the molar heat capacity, enthalpy $(H_T - H_{298.15})$, and entropy $(S_T - S_{298.15})$ increase with the increase of temperature, while the change of free energy $(G_T - G_{298.15})$ is just the opposite. The variations of $(H_T - H_{298.15})$, $(S_T - S_{298.15})$, and $(G_T - G_{298.15})$ with T are plotted in Figure 4.

4. Conclusions

In the work, pinnoite and inderite have been successfully synthesized and characterized, and then the solid molar heat capacities of $MgB_2O_4 \cdot 3H_2O$ and $Mg_2B_6O_{11} \cdot 15H_2O$ were measured by differential scanning calorimetry. The experimental results showed that the molar heat capacities of the two magnesium borates are increased with the increase of temperature. No phase transitions or other thermal anomalies occurred. At the same time, heat capacity at various temperatures was fitted by the least-square method, and the polynomial equation of the change of the molar heat capacity with the temperature is obtained. The fitting results are in good agreement with the experimental data and can be used for the exploitation and utilization of magnesium and boron resources in salt lakes.

Data Availability

The data used to support the findings of this study are available from the corresponding author upon request.

Conflicts of Interest

The authors declare that they have no conflicts of interest.

Acknowledgments

Financial supports from the National Natural Science Foundation of China (21773170 and U1607123), the Key Projects of Natural Science Foundation of Tianjin (18JCZDJC10040), and the Yangtze Scholars and Innovative Research Team in Chinese University (IRT_17R81) are acknowledged.

References

[1] D. L. Shen, X. P. Yu, Y. F. Guo, S. Q. Wang, and T. L. Deng, "Boron and its compounds in new energy and materials fields," *Applied Mechanics and Materials*, vol. 71–78, pp. 2594–2597, 2011.

[2] W. G. Fahrenholtz, E. W. Neuman, H. J. Brown-Shaklee, and G. E. Hilmas, "Superhard boride-carbide particulate composites," *Journal of the American Ceramic Society*, vol. 93, no. 11, pp. 3580–3583, 2010.

[3] D. H. Zhou, T. Sun, and L. Q. Bai, "Experimental study on improving the quality of sintered ore by boron-containing additives," *Journal of Northeastern University*, vol. 25, no. 5, pp. 439–441, 2004.

[4] T. Tan, "Application of superconducting magnesium diboride (MGB2) in superconducting radio frequency cavities," Doctoral dissertation, Temple University, Philadelphia, USA, 2015.

[5] S. Y. Gao, P. S. Song, S. P. Xia et al., *Chemistry of Salt Lake: A New Type of Boron and Lithium Salt Lake*, Science Press, Beijing, China, 2007.

[6] B. W. Luo, T. L. Deng, D. Li, and J. Gao, "Kinetics studies on natural salt minerals of magnesium borates," *World Science-Technology Research and Development*, vol. 33, no. 2, pp. 278–283, 2011.

[7] Q. Li, *Synthesis of Octopirox Intermediate 4–methyl–6–(2,4,4–trimetylpentyl)–2–Pyrone and Measurement of Correlated Heat Capacities*, Zhejiang University, Hangzhou, China, 2010.

[8] M. A. Bespyatov, I. S. Chernyaikin, V. N. Naumov, P. A. Stabnikov, and N. V. Gelfond, "Low-temperature heat capacity of $Al(C_{11}H_{19}O_2)_3$," *Thermochimica Acta*, vol. 596, no. 29, pp. 40-41, 2014.

[9] W. Cui, L. Li, Y. Guo, S. Zhang, and T. Deng, "Heat capacity and thermodynamic property of lithium pentaborate pentahydrate," *Journal of Chemistry*, vol. 2018, no. 6, Article ID 7962739, 4 pages, 2018.

[10] P. S. Gill, S. R. Sauerbrunn, and M. Reading, "Modulated differential scanning calorimetry," *Journal of Thermal Analysis*, vol. 40, no. 3, pp. 931–939, 1993.

[11] F. Li, S. S. Zhang, Y. F. Guo, S. Q. Wang, and T. L. Deng, "Study on a rapid synthetic method for inderite," *China Science Paper*, vol. 9, no. 9, pp. 1080–1082, 2014, in Chinese.

[12] F. Li, S. S. Zhang, Y. F. Guo, S. Q. Wang, and T. L. Deng, "A rapid synthetic method for inderite," *Acta Geologica Sinica*, vol. 88, no. 1, pp. 343-344, 2014.

[13] R. L. Frost and Y. Xi, "Vibrational spectroscopy of the borate mineral pinnoite $MgB_2O(OH)_6$," *Spectrochimica Acta Part A: Molecular and Biomolecular Spectroscopy*, vol. 117, pp. 428–433, 2014.

[14] H. W. Ge, Y. Yao, and T. L. Deng, "Study of improvement on mass titration of borate in brine," *Chemical Research and Application*, vol. 29, no. 1, pp. 112–117, 2017.
[15] J. G. Speight and N. A. Lange, *Lange's Handbook of Chemistry False*, McGraw–Hill, New York, NY, USA, 16th edition, 2005.
[16] J. Guo, "Superficially analyzes that differential scanning calorimetry mensurates the specific heat capacity of the material," *Sci-Tech Innovation and Productivity*, vol. 165, no. 10, pp. 19-20, 2007.